

A ResNet-Based Attention Network for Hyperbola Recognition in Ground-Penetrating Radargrams

Hang Ye, Ai Yang, Jiahao Luo, Miansi Li and Dongguo Zhou

Abstract—As a non-destructive examination tool, ground penetrating radar (GPR) is essential for locating subsurface items and illuminating the underground environment. Unfortunately, there is still work to be done in the practical application of automatic detection of subsurface objects in the radargram. The most frequent targets for their detection are those that resemble cylinders. A buried cylinder is known to produce a hyperbolic signature in GPR images. For the purpose of recognizing subsurface cylinders using GPR data, a novel approach is proposed. The approach makes use of both the strengths of the ResNet model and the characteristics of the hyperbolic curve. Specifically, by introducing priori knowledge and inception modules into the ResNet framework, the suggested method obtains a significant improvement in terms of object recognition at a very low computation cost. At the same time, a hyperparameter optimization strategy is also provided for model training. The evaluations by comparison with other modules demonstrate the effectiveness of the proposed method.

Index Terms—ground penetrating radar, attentional mechanism, neural network, pattern recognition

I. INTRODUCTION

THE ground penetrating radar (GPR) is one of the most popular instruments for inspecting objects close to the surface. As a very effective and non-destructive method, GPR inspection is applicable to a variety of fields, including geological survey [1], civil engineering [2], military target detection [3], and so on. With the expansion of its application field, it is urgent to increase the accuracy and automation of target detection [4].

In general, the whole process of target detection in the GPR image can be divided into three stages: region selection,

feature extraction, and object recognition [5]. Among them, feature extraction is the crucial, critical step. Hyperbolas in the GPR image are typically signatures generated by landmines, cables, pipes, rebars, or tree roots [6]. As a result, our research focuses on the detection of hyperbolas.

Despite significant research efforts over the past two decades, there are still no reliable algorithms for feature extraction from GPR data [7]. This is partly due to the fact that GPR data can be distorted by such environmental factors as soil moisture, rough surface scattering, and subsurface heterogeneity [8]. Additionally, as soil depth increases, an object's GPR signal becomes progressively weaker and, in some cases, completely obscured by background noise, making the recognizer susceptible to error. Especially for GPRs with unshielded antennas, energy can go into the air besides the ground. Consequently, reflections from anything above ground, such as walls, cars, fences, or overhead cables, can act as a source of interference.

To alleviate this problem, machine learning techniques were employed for GPR inspection. However, for neural networks with shallow architecture, feature extraction is a challenging task [7], while, deep learning techniques (DL) [7, 9-11] naturally incorporate low-, medium-, and high-level features and hence gain more and more attention. Undoubtedly, DL methods provide a universal and brilliant solution for classification and regression tasks, especially when used on large datasets [12-14]. However, the inadequate supply of training data degrades the performance of these conventional approaches [15]. At the same time, for GPR image, large sample sets are expensive and time-consuming.

Furthermore, the desirable performance of DL methods usually tends to be achieved at the cost of computational complexity [16]. They are therefore frequently inappropriate for real-time tasks.

On the other hand, a universal model such as a neural network tends to be somewhat unsuccessful for a specific task according to “no free lunch” theorems [17]. In order to detect the subsurface cylinder in this instance, an exclusive neural network is created, especially for limited data sets.

With these considerations in mind, a smart and lightweight approach is being explored for the recognition of subsurface cylinders from GPR data. The method leverages the advantages of the ResNet model and the features of cylindrical objects. Specifically, the primary contributions of this paper can be summarized as follows:

- (1) selecting and expressing a subsurface cylinder feature;
- (2) creating a neural network frame with an attention

Manuscript received April 27, 2022; revised January 30, 2023.

This work was supported by Science and technology project of China Southern Power Grid Co., LTD (grant No. GDKJXM20198168).

Hang Ye is a project manager of Marketing Service Center of Guangdong Power Grid Corporation of China Southern Power Grid, Heyuan 517000, China (phone: 17783700156; e-mail: 385035723@qq.com).

Ai Yang is a project executive of Marketing Service Center of Guangdong Power Grid Corporation of China Southern Power Grid, Heyuan 517000, China (e-mail: adolake@hotmail.com).

Jiahao Luo is a data analyst of Marketing Service Center of Guangdong Power Grid Corporation of China Southern Power Grid, Heyuan 517000, China (e-mail: 329101854@qq.com).

Miansi Li is a research assistant of Marketing Service Center of Guangdong Power Grid Corporation of China Southern Power Grid, Heyuan 517000, China (e-mail: maxwell201904@163.com).

Dongguo Zhou is a lecturer of Wuhan University, Wuhan 430077, China (e-mail: zdg20042586@163.com).

mechanism for the hyperbola recognition task;

(3) exploring the impact of hyperparameters on neural network training;

(4) conducting extensive experiments to evaluate the method's efficacy.

The remainder of the paper is structured as follows. Section II reviews related work. Section III introduces our framework of hyperbola recognition, while Section IV describes the proposed model based on the ResNet network. Section V shows the experimental results. Finally, Section VI states the conclusions.

II. RELATED WORK

When an electromagnetic wave is radiated from a transmitting antenna and hits a buried object such as a pipe, the wave is reflected to the surface and captured by a receiving antenna. The time-history of a single pulse's movement from the transmit antenna to the receive antenna is called a "trace" [18]. A single trace, that is, recording data collected at a single point, is referred to as an A-scan imaging. In contrast, when a downward-looking GPR antenna is moved along a straight path on the top of the surface, the trace acquired at different spatial positions is known as a B-scan imaging [19]. A cylinder-like object perpendicular to the measured line is typically depicted in the B-scan image as a hyperbola pattern [20]. In this sense, the hyperbolic pattern is the typical feature used to detect cylindrical targets [21].

To detect cylindrical targets, the hyperbolic signatures on the B-scan image are frequently formulated as a geometric model [22]. A hyperbola can then be fitted easily with GPR data. In order to recognize hyperbola and determine the location of the targets as well as the relative permittivity of the medium, Al-Nuaimy et al. [23] presented a coarse-to-fine fitting method. A probabilistic model was given by Chen and Cohn [24] to fit hyperbola. Another fitting method based on the Hough transform was offered by Maas and Christian [25]. To improve the efficacy of hyperbola detection, Borgioli et al. [26] enhanced the Hough transform by introducing a weighting factor.

In addition, Delbo et al. [27] suggested a pattern recognition approach based on fuzzy clustering to detect hyperbolic signatures. Based on support vector machine (SVM), Pasolli et al. [28] proposed a novel system of pattern recognition to classify cylindrical objects. By adopting SVM, the accuracy of rebar detection can reach 91.5%-92.45% [29]. On the other hand, Sagnard and Tarel [30] devised a template-matching algorithm to detect hyperbola in ground-penetrating radargrams.

However, cylinder-like objects are not always strictly hyperbolic in radar images because of the heterogeneity of the medium and reciprocal interactions of radar waves. The hyperbola pattern has too many variations for accurate recognition in natural situations.

To alleviate this problem, recent studies have employed deep learning frameworks for hyperbola detection. Deep learning allows computational models with multiple processing layers to automatically learn the representation of abstract features [31]. Xiang et al. [32] adopted AlexNet to

detect rebars from small patches of GPR images. By means of Faster R-CNN, Lei et al. [33] achieved an accuracy of 92.13% after 3000 iterations. Ozkaya and Seyfi [34] explored a multilevel deep dictionary learning algorithm with the classification accuracy of 94.4%. The classification method of Ishitsuka et al. [35] obtained the accuracy of 94.5%-97.9% by using a convolutional neural network (CNN).

In conclusion, despite considerable effort over the past two decades, hyperbolic detection in radargrams is still an open problem. The researchers have drawn on this end from various areas, reliable hyperbolic detection has proved an elusive goal. There is still substantial room for improvement.

III. PROPOSED METHOD

A B-scan image is a 2D (depth, down-track) image that represents a vertical slice of the ground. When a subterranean cylinder is perpendicular to the slice, its profile in the radargram is a hyperbolic curve. In this section, we will introduce our methodology and framework for hyperbola detection in the B-scan image.

A. Methodology of Hyperbola Detection

Due to the fact that the curvature of hyperbola varies continuously and regularly, and edge points as well as their curvature are the key features of target detection, along with original data, edge points and edge direction are fed into the neural network to estimate parameters of the model and to detect hyperbola.

Owing to the brilliant performance at the ILSVRC (2015) competition and wide success in many application fields [36], the ResNet model is employed as the basic network structure for hyperbola detection. Indeed, the ResNet model was initially investigated for RGB images [37], which completely differ from GPR images in the physical property sense.

Unlike RGB images, where one channel is similar to the others, every channel of input data is distinct from each other for GPR images. Each input channel has a separately contribution to recognition tasks. For this reason, it is necessary to assess the weight for each channel individually.

In order to improve performance, we included an attentional mechanism to the ResNet framework, which was inspired by a neuroscience model of the primate visual cortex.

In other words, the paper suggests an integrated method combining domain knowledge, attention mechanism, and ResNet neural network for hyperbola detection in the B-scan image. The modified ResNet framework will be described in detail in Section IV.

B. Hyperbola Detection Process

Based on the properties of the hyperbola curve and deep learning, this paper provides a hyperbola detector that goes through the following four steps.

Step 1: Edge Strength Estimation

To save computational cost, a fixed-size window is used here. Given an image I , the edge strength can be estimated in a 2×2 window by the magnitude of S as follows [38].

$$S = \sqrt{(G_x * I)^2 + (G_y * I)^2} \quad (1)$$

where * denotes convolution, and

$$G_x = \frac{1}{2} \begin{bmatrix} -1 & 1 \\ -1 & 1 \end{bmatrix} \quad (2)$$

$$G_y = \frac{1}{2} \begin{bmatrix} 1 & 1 \\ -1 & -1 \end{bmatrix} \quad (3)$$

In practice, we may move the 2×2 block across a picture from top to bottom and from left to right to get the edge strength of every pixel. Zero padding is utilized in this instance to ensure that the output is the same size as the input.

Step 2: Edge Direction Estimation

In a similar way, the edge direction at each pixel can be computed by

$$\alpha = \begin{cases} \frac{\pi}{2} & \text{if } G_x * I = 0 \\ \arctan\left(\frac{G_y * I}{G_x * I}\right) & \text{else} \end{cases} \quad (4)$$

It is worth noting that computational costs can be reduced by merely sharing the $G_y * I$ and $G_x * I$ results in Steps 1 and 2 at very low memory space costs.

Step 3: Training the Proposed Model

In the model training process, transfer learning is utilized to get the optimal model parameters. Additionally, the Ray Tune framework [39], which is the hyperparameter library building on top of the Ray distributed computing framework, is used to carry out hyperparameter optimization. Specifically, the ResNet-based network model is pre-trained on the ImageNet data set beforehand so that the weights produced can be used as the initial estimation of the model parameters [40]. The model, which is described in detail in Section IV, is then retrained on the GPR data using the self-adaptive gradient descent algorithm [41].

Although data augmentation might help the network model perform better, most of augmentation techniques are not appropriate for the GPR data. Fortunately, vertical flips are still effective. However, a horizontal flip is invalid since the outcome has a different physical meaning than the original image.

Step 4: Hyperbola Recognition

To introduce the hyperbolic curve features into the ResNet model, GPR data are pre-processed by the operators mentioned in Step 1 and 2. Combined them with the raw GPR data, the input data is constructed with three channels. Then, the 3-channel data is fed into the network model. By explicitly modelling independence between channels, channel-wise feature responses can be adaptively recalibrated, which can speed up the learning process and considerably increase the network's capacity for representation [42].

In the prediction phrase, we may determine the likelihood that the image contains a hyperbola after forward propagation computing. The prediction result is the case if it is more than 0.5.

helpful to know the attributes of the ResNet model. The model typically has stacked convolutional layers followed by one or more fully connected layers. At the ILSVRC (2015) classification competition, the ResNet model outperformed all the others [37]. The following provides an explanation for why this model is superior:

1) The vanishing gradient problem is addressed using residual modules, which prevent the model from exponentially expanding into distinct sub-networks [43];

2) Overfitting is avoided by using a shortcut connection, which gives the user the option of arming the network with trainable weights or not;

3) Immunity to noise is enhanced with the use of pooling operations, so that the output is steady even if the input is fluctuant.

Though the ResNet model works well on RGB images, it still needs to be modified for GPR data due to their different characteristics. In addition, the ResNet model does not permit input data sizes smaller than 112 [37]. Unfortunately, GPR images are usually small in size.

On the other hand, each channel has unique qualities from the others. For example, a GPR image channel is continuous in intensity. On the contrary, edge strength and edge direction channels are discontinuous. Furthermore, each channel contributes differently to the recognition task. In this regard, a channel-wise CNN should be employed. The three channels are not, however, totally independent of one another.

Based on the above considerations, the first convolution layer is substituted with the inception module proposed by Szegedy et al. [44], which can be used as a drop-in replacement for the original block. In order to reduce model complexity and widen the scope of applications, this module

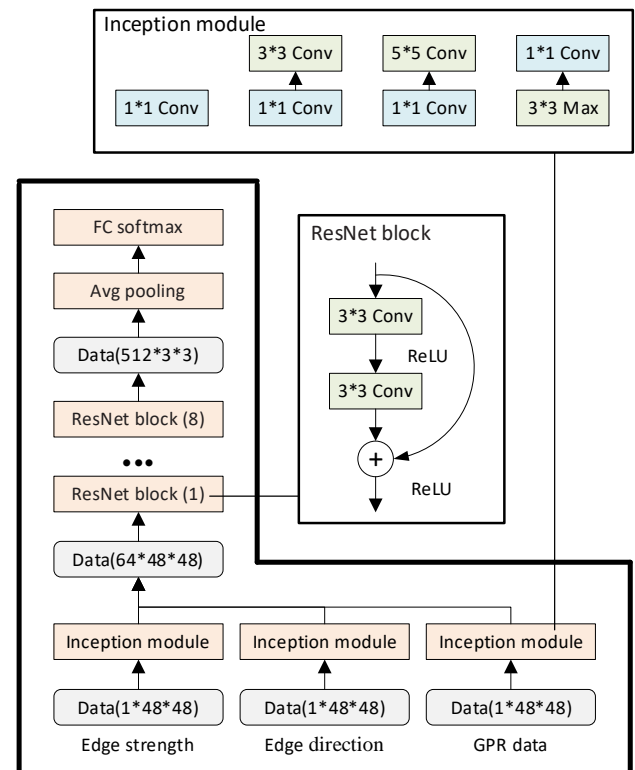


Fig. 1. ResNet-based attention network. Here, Conv, Max and FC indicate convolution, max pooling and full connection, respectively.

IV. IMPROVED RESNET MODEL

Prior to providing a full explanation of the model, it is

doesn't get inserted into the other building blocks of the ResNet model, and downsampling operations are removed. Furthermore, a full connection layer with the Softmax function is used for the purpose of hyperbola detection.

Admittedly, the deeper a model network is, the better its performance is. However, the 18-layer ResNet can still obtain comparable accuracy. Furthermore, it converges more quickly than deeper networks [37]. This makes it possible to use the model in a real-time system. As a result, the full model is constructed using both the inception module and the 18-layer ResNet-based framework, as illustrated in Fig. 1. Notice that every ResNet block consists of two convolution layers, and each inception module includes six convolution operators and a max-pooling layer.

For training and testing data, the weighted binary cross-entropy [45] is employed as a loss function. In the training process, the mini-batch gradient descent with momentum is applied to optimise the cross-entropy loss of the Softmax classifier [46]. Moreover, a vertical flip is performed for each image in the training set.

V. EXPERIMENTAL RESULTS

In this section, we present our evaluation methodology and results from the real GPR data. The performance of the attention network built on ResNet is evaluated and compared with other models.

To ensure extensibility, the Python language is used to implement the algorithm proposed here. The libraries PyTorch [47] and Ray Tune [39] are employed in the programming process. To save training time, we opted for a straightforward and practical hyperparameter optimization technique, Asynchronous Successive Halving Algorithm [48], which is suitable for massive parallelism and takes advantage of early stopping.

To test our model, we used the dataset DECKGPRH1.0, which was cropped by Asadi et al. [49] from GPR field data of

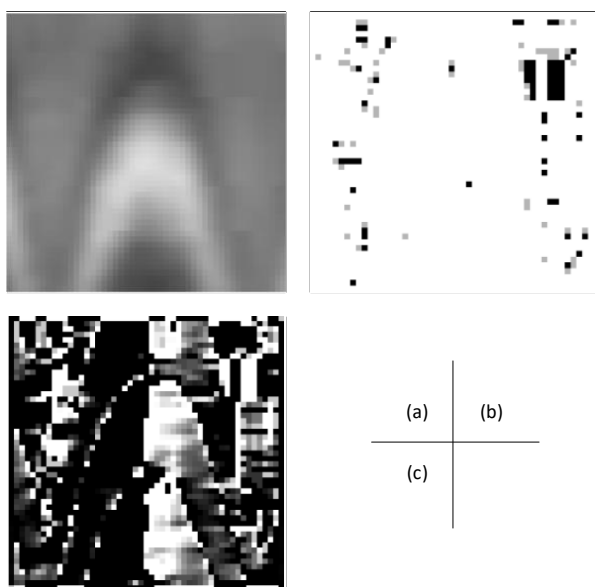


Fig. 2. The 3-channel input data: (a) GPR data; (b) edge strength; (c) edge direction.

a real bridge deck. The dataset contains 16,876 B-scan images. In the dataset, there are 8436 negative samples and 8440 positive samples. Here, half of them are used for testing and half for training.

We conducted all of our experiments using the Ray Framework on a Linux PC with one Nvidia 3080Ti GPU and 16 CPUs running at a maximum frequency of 3.9 GHz.

Fig. 2 illustrates a sample of the 3-channel pre-processed dataset, i.e., the GPR data and the corresponding results after executing the operators described in Step 1 and 2. Here, every channel of input data is a 48×48 matrix. All the positive samples are placed in one folder and the negative samples in the other. In this way, it is easy to judge whether there is a hyperbola in the radargram according to the corresponding folder.

For a fair comparison, we defined the exact same configuration spaces for each method. With uniformly sampling the hyperparameters, each method picked up 20 samples in the hyperparameter spaces. In the training process, the learning rate is treated as an exponential random variable with a range of 0 to 0.5. Momentum ranges from 0.1 to 0.9 and follows a random distribution. There is a total of 20 trials, and their hyperparameters are listed in Table I.

TABLE I
SAMPLES IN THE HYPERPARAMETER SPACES FOR ALL ALGORITHMS

Number	Learning rate	Momentum
1	5.86207e-09	0.835338
2	0.4045427	0.889455
3	4.8015e-05	0.734375
4	0.4821682	0.674546
5	5.35385e-09	0.496728
6	4.28036e-06	0.756512
7	0.1922548	0.484825
8	0.0117198	0.809185
9	2.06086e-07	0.536543
10	6.96564e-10	0.546641
11	4.77752e-08	0.457425
12	2.7343e-09	0.534873
13	3.23298e-05	0.874085
14	0.03530775	0.527668
15	2.53252e-10	0.875159
16	0.1180631	0.626482
17	1.1586e-08	0.645687
18	9.3285e-07	0.242596
19	6.16827e-05	0.562090
20	5.03267e-06	0.358555

Figure 3 depicts the results at various levels of momentum and learning rate. Yellow points in the image indicate high accuracy. It is clear that high accuracy results are obtained at a low learning rate, whereas momentum is not clearly related to the results.

In our experiments, we investigated alternative techniques on the canonical ResNet model. For instance, we attempted to use maximum pooling rather than average pooling. Unfortunately, it produces poorer results than simple averaging.

Due to the early-stopping technique in the Ray Tune architecture, most trial runs are terminated after one epoch, i.e., a full pass over the data set, which includes 132 batches. That means that the parameters should be updated 132 times per epoch. For all of the samples in the hyperparameter space, the values of the corresponding loss function are displayed in

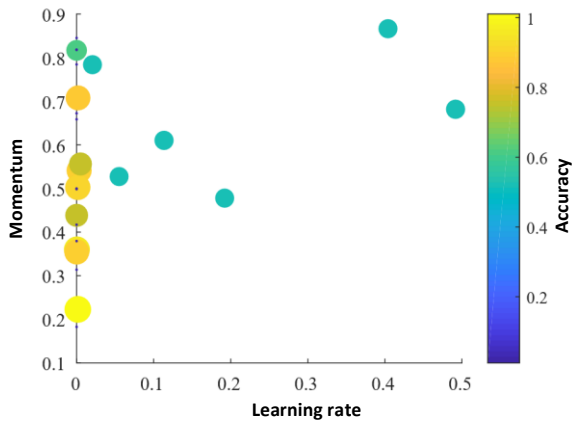


Fig. 3. Accuracy of the results at various levels of momentums and learning rates.

Fig. 4. Every epoch's accuracy is shown in Fig. 5. Every trial is depicted with a different color. Note that the total number of trials is 20 and some points are overlapping in the image.

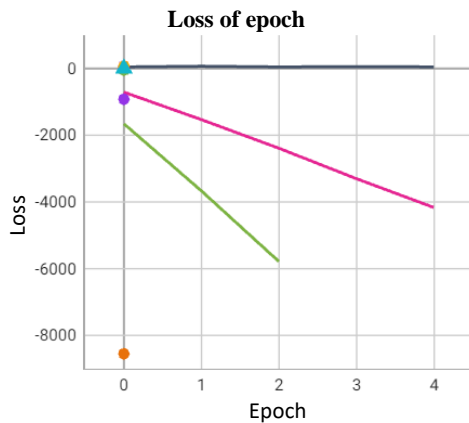


Fig. 4. The loss values of the epochs for all parameter configurations.

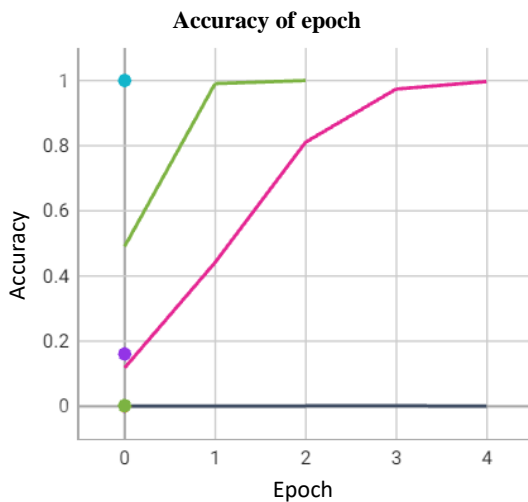


Fig. 5. The accuracy values of the epochs for all parameter configurations.

To evaluate performance, the model proposed here is tested and compared to state-of-the-art models using the GPR data. Considering the fact that some models, such as VGG [50] and ResNet [37], share the same style of samples, while others, such as the RCNN [51] family, work with different label styles, experimental comparison is limited to the models

which can run on the same data.

As a result, we compare our model to LeNet [52], AlexNet [53], VGG [50], and ResNet [37] under identical conditions in terms of the mean processing time per iteration and recognition accuracy (the percentage of the images with correct classification, i.e., the number of the correctly classified images divided by the total number of the testing images).

To compare all methods fairly, we selected the parameters that produced the best result in 20 trials for each model. Because learning rate has a significant impact on trained model accuracy, the learning rate schedule used here is the conventional annealing method with warmup, i.e., a strategy of using lower learning rates at the start of training to overcome early optimization difficulties [54].

The results of the comparative test are tabulated in Table II. Here, accuracy is determined by the best result in 20 trials. The time in Table II represents the average processing time per iteration with a batch size of 64. It is readily seen that the proposed model is better than the others in terms of recognition accuracy. The processing time is slightly longer than the others, but it is very close. In the experiments, VGG and ResNet consist of 11 and 18 layers, respectively. And, the proposed model here is also based on the 18-layer ResNet network.

TABLE II
COMPARISON OF PERFORMANCE BETWEEN THE PROPOSED MODEL AND SOME STATE-OF-THE-ART MODELS

Model	Accuracy	Time(s)
LeNet	0.897	6.61
AlexNet	0.814	6.78
VGG	0.905	6.74
ResNet	0.963	6.83
Proposed model	0.991	6.97

Note: Accuracy in this table means the percentage of the images with correct classification; Time is the mean running time per iteration.

VI. CONCLUSION

In this work, we investigated the ResNet architecture and hyperbola characteristics. Based on the findings, a light-weight model is proposed to recognize hyperbola in GPR data. By adopting the integration of prior knowledge and the inception module, the proposed network model achieves high accuracy in the comparative experiment relative to four state-of-the-art models at very low computational costs. In addition, hyperparameter optimization strategy and experience are discussed in this paper.

In conclusion, a light-weight model is presented exclusively for hyperbola recognition in GPR images. Its performance outperforms that of the canonical models. The proposed network model has a wide range of applications in a real-time system for a variety of purposes, such as the detection of pipelines in the soil and rebars in the concrete structure. The successful application of the inception architecture can serve as a reference for deep learning researchers and practitioners.

ACKNOWLEDGMENT

Most ideas in this paper have taken shape as part of a long collaboration with the scholars at Wuhan University. The scholars at Chongqing University of Posts and Telecommunications also helped us by sharing their ideas on knowledge introduction long before it was published.

REFERENCES

- [1] J. L. Davis and A. P. Annan, "Ground-penetrating radar for high-resolution mapping of soil and rock stratigraphy," *Geophys. Prospect.*, vol. 37, no. 5, pp. 531-551, 1989.
- [2] I. Morris, H. Abdel-Jaber and B. Glisic, "Quantitative attribute analyses with ground penetrating radar for infrastructure assessments and structural health monitoring," *Sensors*, vol. 19, no. 7, pp. 1-17, 2019.
- [3] P. D. Gader, M. Mystkowski and Y. Zhao, "Landmine detection with ground penetrating radar using hidden Markov models," *IEEE Trans. Geosci. Remote*, vol. 39, no. 6, pp. 1231-1244, 2001.
- [4] Y. Li, Z. Zhao, Y. Luo and Z. Qiu, "Real-Time pattern-recognition of GPR Images with YOLO v3 implemented by TensorFlow," *Sensors*, vol. 20, no. 22, pp. 1-18, 2020.
- [5] K. C. Ho, L. Carin, P. D. Gader and J. N. Wilson, "An investigation of using the spectral characteristics from ground penetrating radar for landmine/clutter discrimination," *IEEE Trans. Geosci. Remote*, vol. 46, no. 4, pp. 1177-1191, 2008.
- [6] X. Zhang, F. Xue, Z. Wang, J. Wen, C. Guan, F. Wang, et al., "A novel method of hyperbola recognition in ground penetrating radar (GPR) B-scan image for tree roots detection," *Forests*, vol. 12, no. 8, pp. 1-25, 2021.
- [7] Z. Tong, J. Gao and D. Yuan, "Advances of deep learning applications in ground-penetrating radar: a survey," *Constr. Build. Mater.*, vol. 258, pp. 1-14, 2020.
- [8] L. Gurel and U. Oguz, "Simulations of ground-penetrating radars over lossy and heterogeneous grounds," *IEEE Trans. Geosci. Remote*, vol. 39, no. 6, pp. 1190-1197, 2001.
- [9] H. Li, N. Li, R. Wu, H. Wang, Z. Gui and D. Song, "GPR-RCNN: an algorithm of subsurface defect detection for airport runway based on GPR," *IEEE Robot. Autom. Lett.*, vol. 6, no. 2, pp. 3001-3008, 2021.
- [10] U. Ozkaya, F. Melgani, M. B. Bejiga, L. Seyfi and M. Donelli, "GPR B scan image analysis with deep learning methods," *Measurement*, vol. 165, pp. 1-9, 2020.
- [11] X. Zhang, L. Han, M. Robinson and A. Gallagher, "A GANs-based deep learning framework for automatic subsurface object recognition from ground penetrating radar data," *IEEE Access*, vol. PP, no. 99, pp. 1-10, 2021.
- [12] I. Goodfellow, Y. Bengio and A. Courville. *Deep learning*. City, MIT press, 2016.
- [13] Y. Liu, M. Yang, J. Li, Q. Zheng and D. Wang, "Dynamic hand gesture recognition using 2D convolutional neural network," *Engineering Letters*, vol. 28, no. 1, pp. 243-254, 2020.
- [14] Z. Hu, S. Tang, Y. Luo, F. Jian and X. Si, "3DACRNN model based on residual network for speech emotion classification," *Engineering Letters*, vol. 29, no. 2, pp. 400-407, 2021.
- [15] G. C. Cawley and N. L. Talbot, "On over-fitting in model selection and subsequent selection bias in performance evaluation," *J. Mach. Learn Res.*, vol. 11, pp. 2079-2107, 2010.
- [16] G. B. Huang, H. Zhou, X. Ding and R. Zhang, "Extreme learning machine for regression and multiclass classification," *IEEE Trans. Syst. Man Cyb.*, vol. 42, no. 2, pp. 513-529, 2011.
- [17] D. H. Wolpert and W. G. Macready, "No free lunch theorems for optimization," *IEEE Trans. Evolut. Comput.*, vol. 1, no. 1, pp. 67-82, 1997.
- [18] D. J. Daniels. *Ground penetrating radar*. City, The Institution of Electrical Engineer, 2004.
- [19] M. Moalla, H. Frigui, A. Karem and A. Bouzid, "Application of convolutional and recurrent neural networks for buried threat detection using ground penetrating radar data," *IEEE Trans. Geosci. Remote*, vol. 58, no. 10, pp. 7022-7034, 2020.
- [20] P. Zhang, L. Shen, T. Wen, X. Huang and Q. Xin, "Vector phase symmetry for stable hyperbola detection in ground-penetrating radar images," *IEEE Trans. Geosci. Remote*, vol. 60, pp. 1-12, 2022.
- [21] H. Ali, N. S. M. Ideris, A. A. Zaidi, M. Z. Azalan, T. T. Amran, M. Ahmad, et al., "Ground penetrating radar for buried utilities detection and mapping: a review," *Journal of Physics: Conference Series*, 2021, pp. 1-9.
- [22] X. Zhou, Q. Chen, S. Lyu and H. Chen, "Mapping the buried cable by ground penetrating radar and Gaussian-process regression," *IEEE Trans. Geosci. Remote*, vol. 60, pp. 1-10, 2022.
- [23] W. Al-Nuaimy, Y. Huang and A. Eriksen, "Automatic detection of hyperbolic signatures in ground-penetrating radar data," *Subsurface and surface sensing technologies and applications III*, 2001, pp. 327-335.
- [24] H. Chen and A. G. Cohn, "Probabilistic robust hyperbola mixture model for interpreting ground penetrating radar data," *The 2010 International Joint Conference on Neural Networks (IJCNN)*, Barcelona, Spain, 2010, pp. 1-8.
- [25] C. Maas and J. Schmalzl, "Using pattern recognition to automatically localize reflection hyperbolas in data from ground penetrating radar," *Comput. Geosci-uk.*, vol. 58, pp. 116-125, 2013.
- [26] G. Borgioli, L. Capineri, P. Falorni, S. Matucci and C. G. Windsor, "The detection of buried pipes from time-of-flight radar data," *IEEE Trans. Geosci. Remote*, vol. 46, no. 8, pp. 2254-2266, 2008.
- [27] S. Delbo, P. Gamba and D. Roccatto, "A fuzzy shell clustering approach to recognize hyperbolic signatures in subsurface radar images," *IEEE Trans. Geosci. Remote*, vol. 38, no. 3, pp. 1447-1451, 2000.
- [28] E. Pasolli, F. Melgani and M. Donelli, "Automatic analysis of GPR images: a pattern-recognition approach," *IEEE Trans. Geosci. Remote*, vol. 47, no. 7, pp. 2206-2217, 2009.
- [29] P. Kaur, K. J. Dana, F. A. Romero and N. Gucunski, "Automated GPR rebar analysis for robotic bridge deck evaluation," *IEEE Trans. Cybernetics*, vol. 46, no. 10, pp. 2265-2276, 2016.
- [30] F. Sagnard and J.-P. Tarel, "Template-matching based detection of hyperbolas in ground-penetrating radargrams for buried utilities," *J. Geophys. Eng.*, vol. 13, no. 4, pp. 491-504, 2016.
- [31] Y. LeCun, Y. Bengio and G. Hinton, "Deep learning," *Nature*, vol. 521, no. 7553, pp. 436-444, 2015.
- [32] Z. Xiang and A. Rashidi, "An improved convolutional neural network system for automatically detecting rebar in GPR data," *Int. Conf. Comput. Civil. Eng.*, Atlanta, USA, 2019, pp. 422-429.
- [33] W. Lei, F. Hou, J. Xi, Q. Tan, M. Xu, X. Jiang, et al., "Automatic hyperbola detection and fitting in GPR B-scan image," *Automat. Constr.*, vol. 106, pp. 1-14, 2019.
- [34] U. Ozkaya and L. Seyfi, "Deep dictionary learning application in GPR B-scan images," *Signal Image Video P.*, vol. 12, no. 8, pp. 1567-1575, 2018.
- [35] K. Ishitsuka, S. Iso, K. Onishi and T. Matsuoka, "Object detection in ground-penetrating radar images using a deep convolutional neural network and image set preparation by migration," *Int. J. Geophys.*, vol. 2018, pp. 1-9, 2018.
- [36] N. Hnoohom, S. Mekruksavanich and A. Jitpattanakul, "An efficient ResNetSE architecture for smoking activity recognition from smartwatch," *Intell. Autom. Soft Comput.*, vol. 35, no. 1, pp. 1245-1259, 2023.
- [37] K. He, X. Zhang, S. Ren and J. Sun, "Deep residual learning for image recognition," *P. IEEE conf. comput. vision pattern recogn.*, Las Vegas, USA, 2016, pp. 770-778.
- [38] J. Canny, "A computational approach to edge detection," *IEEE Trans. Pattern Anal. Mach. Intell.*, vol. 8, no. 6, pp. 679-698, 1986.
- [39] R. Liaw, E. Liang, R. Nishihara, P. Moritz, J. E. Gonzalez and I. Stoica, "Tune: a research platform for distributed model selection and training," *arXiv*, pp. 1-8, 2018.
- [40] S. J. Pan and Y. Qiang, "A survey on transfer learning," *IEEE Trans. Knowl. Data Eng.*, vol. 22, no. 10, pp. 1345-1359, 2010.
- [41] Y. Xue, Y. Wang and J. Liang, "A self-adaptive gradient descent search algorithm for fully-connected neural networks," *Neurocomputing*, vol. 478, pp. 70-80, 2022.
- [42] H. Jie, S. Li, S. Gang and S. Albanie, "Squeeze-and-excitation networks," *IEEE Trans. Pattern Anal. Mach. Intell.*, vol. 42, no. 8, pp. 2011-2023, 2020.
- [43] Z. Wu, C. Shen and A. Van Den Hengel, "Wider or deeper: revisiting the ResNet model for visual recognition," *Pattern Recogn.*, vol. 90, pp. 119-133, 2019.
- [44] C. Szegedy, W. Liu, Y. Jia, P. Sermanet, S. Reed, D. Anguelov, et al., "Going deeper with convolutions," *P. IEEE conf. comput. vision pattern recogn*, Boston, MA, 2015, pp. 1-9.
- [45] Z. Bai, J. Wang, X. L. Zhang and J. Chen, "End-to-end speaker verification via curriculum bipartite ranking weighted binary cross-entropy," *IEEE Trans. Audio, Speech, Language Process.*, vol. 30, pp. 1330-1344, 2022.
- [46] S. A. Ebiaredoh-Mienye, E. Esenogho and T. G. Swart, "Integrating enhanced sparse autoencoder-based artificial neural network technique

- and Softmax regression for medical diagnosis," *Electronics*, vol. 9, no. 11, pp. 1963, 2020.
- [47] A. Paszke, S. Gross, F. Massa, A. Lerer, J. Bradbury, G. Chanan, et al., "Pytorch: an imperative style, high-performance deep learning library," *Advances in neural information processing systems*, vol. 32, pp. 1-12, 2019.
- [48] L. Li, K. Jamieson, A. Rostamizadeh, E. Gonina, J. Ben-Tzur, M. Hardt, et al., "A system for massively parallel hyperparameter tuning," *Proceedings of Machine Learning and Systems*, vol. 2, pp. 230-246, 2020.
- [49] P. Asadi, M. Gindy and M. Alvarez, "A machine learning based approach for automatic rebar detection and quantification of deterioration in concrete bridge deck ground penetrating radar B-scan images," *KSCE J. Civil Eng.*, vol. 23, no. 6, pp. 2618-2627, 2019.
- [50] K. Simonyan and A. Zisserman, "Very deep convolutional networks for large-scale image recognition," arXiv, pp. 1-14, 2014.
- [51] K. He, G. Gkioxari, P. Dollár and R. Girshick, "Mask R-CNN," *Proc. IEEE int. conf. comput. vision*, 2017, pp. 2961-2969.
- [52] Y. LeCun, L. Bottou, Y. Bengio and P. Haffner, "Gradient-based learning applied to document recognition," *Proc. IEEE*, vol. 86, no. 11, pp. 2278-2324, 1998.
- [53] A. Krizhevsky, I. Sutskever and G. E. Hinton, "Imagenet classification with deep convolutional neural networks," *Advances in neural information processing systems*, Lake Tahoe, USA, 2012, pp. 1-9.
- [54] P. Goyal, P. Dollár, R. Girshick, P. Noordhuis, L. Wesolowski, A. Kyrola, et al., "Accurate, large minibatch SGD: training ImageNet in 1 hour," arXiv, pp. 2017.

Hang Ye was born in Heyuan, Guangdong Province, China, in 1997. He received his degree in B.E. in Computer Science (2019) at Guangzhou University of Technology. His research topics are focused on electrical power system.